Cormorant-Inspired Macro-Porous Hydrogel Thin Film Evaporators for Boosting Cost-Effective Solar Water Purification

Guang-Lei Ma [a], Xi-Yan Qi [a], Qing-Cong Wei [b], Xiao-Fang Shi [b], Yi Chang [a], Yu-Ming Guo [b], Zhi-Guo Hu* [b], Xiao-Ming Ma* [a]*

[a] Key Laboratory of Green Chemical Media and Reactions, Ministry of Education, School of Chemistry and Chemical Engineering, Henan Normal University, Xinxiang, Henan 453007, China. E-mail: mxm@htu.edu.cn

[b] Collaborative Innovation Center of Henan Province for Green Manufacturing of Fine Chemicals, Henan Engineering Laboratory of Chemical Pharmaceutical and Biomedical Materials, Henan Normal University, Xinxiang, Henan 453007, China. Email: guoyuming@htu.edu.cn, zghu@htu.edu.cn

Cormorant-Inspired Macro-Porous Hydrogel Thin Film Evaporators for Boosting Cost-Effective Solar Water Purification

Guang-Lei Ma, Xi-Yan Qi, Qing-Cong Wei, Xiao-Fang Shi, Yi Chang, Yu-Ming Guo[*], *Zhi-Guo Hu*[*], *Xiao-Ming Ma*[*]

Content

S1. Experimental Section

Chemicals and Materials

Graphite (8000 mesh), LiCl, sodium dodecyl sulfate (SDS), N, N ‘-Methylenebis (2-propenamide) (BIS), lauryl methacrylate (LMA), potassium persulfate (KPS), acrylamide (AAm), N, N, N’, N’-tetramethylethylenediamine (TEMED), acrylic acid (AA), $FeCl_3·H_2O$, and citric acid were purchased from Shanghai Macklin Biochemical Technology Co., Ltd.

Preparation of HAG and HAG-F gels

LiCl (1.6 g) and SDS (0.7 g) were dissolved in 30 ml deionized water and stirred for 10 min. LMA (0.8 g) and graphite (1.5 g) were added and stirred for 3 h at room temperature to disperse. AAm (7.0 g), BIS (0.05 g) were added to the above solution to dissolve completely, and then KPS (0.03 g) and TEMED (15 μL) were added to initiate the reaction. The reaction solution was immediately added to the desired mold and allowed to react overnight at room temperature. Upon completion of polymerization, the gel was removed from the template and immersed in deionized water for 3 days. The polymerization process was completed in the film template to produce HAG-F.

Preparation of IT-HAG and IT-HAG-F gels

LiCl (1.6 g) and SDS (0.7 g) were dissolved in 30 ml deionized water and stirred for 10 min. LMA (0.8 g) and graphite (1.5 g) were added and stirred for 3 h at room temperature to disperse. AAm (7.0 g), BIS (0.05 g) were added to the above solution and pre-cool to 4°C. Then KPS (0.03 g) and TEMED (15 μL) were added and immediately filled the reaction solution into the pre-cooled mold. And the molds were slowly immersed into a -20 °C cold trap for freezing and then placed in a -20 °C refrigerator for 24 h to complete polymerization. After polymerization was completed, the gel was removed from the template and immersed in deionized water for 3 days. The polymerization process was completed in the film template to produce IT-HAG-F.

Preparation of PAAmG

AAm (7.0 g), BIS (0.7 g), SDS (0.7 g), and graphite (1.5 g) were added to 30 ml deionized water and stirred for 10 min, and KPS (0.03 g) and TEMED (15 μL) were added to initiate the reaction. After polymerization was completed, the gel was removed from the template and immersed in deionized water for 3 days.IT-PAAmG and IT-PAAmG were prepared as described above for IT-HAG and IT-HAG-F.

Preparation of FCG

AAm (1.2 g), AA (1 g), BIS (0.01 g), and NaOH (0.56 g) were added to 15 mL deionized water and stirred for 10 min, and APS (0.02 g) and TEMED (50 μL) were added to initiate the reaction. After polymerization was completed, the gel was removed from the template and immersed in aqueous citric acid containing Fe^{3+} for 24 h, and then further immersed in deionized water until no color leaked out.

Preparation of aqueous citric acid solution containing iron ions

Citric acid (19.7 g) was dissolved in 500 mL of deionized water, $FeCl_3 \cdot 6H_2O$ (16.9 g) was added and the solution was made up to pH=4 with NaOH.

Estimation of equivalent evaporation enthalpy

To obtain the enthalpy of evaporation, a controlled experiment was designed to estimate the enthalpy of evaporation. Water and gel samples of equal surface area were synchronized in a closed container along with a supersaturated potassium carbonate solution (to make the humidity stable). The supersaturated potassium carbonate solution was able to stabilize the relative humidity at approximately 45%, and the test was conducted at the temperature at which the IT-HAG-F evaporated (approximately 37 ºC). The water evaporation rate and the corresponding equivalent enthalpy of evaporation (ΔH_{equ}) were calculated using the equation.

$$\Delta H_{vap} m_0 = \Delta H_{equ} m_g \quad 1$$

where ΔH_{vap} and m_0 were the evaporation enthalpy and mass change of bulk water; m_g was the mass change of IT-HAG. The energy efficient was also calculated based on E_{equ}.

Water evaporation performance of different samples under concentrated solar radiation.

The water evaporation performance experiments were conducted using a solar simulator that outputs a simulated solar flux of 1 kW/m^2 (1 sun). The solar flux was measured using a solar power meter. Thin-film gels were measured for evaporation by placing them on different bracket. The mass of water loss was measured using a electronic balance. All tests were performed after 30 min of equilibration.

The corresponding energy efficiency (η) for solar to vapor generation can then be calculated using the following formula:

$$\eta = \dot{m}h_V/C_{opt}P_0 \qquad 2$$

where $\dot{m}$ is the mass flux, h_V is the vaporization enthalpy of the water, P_0 is the solar irradiation power of 1 sun (1 kW·m^{-2}), and C_{opt} refers to the optical concentration on the absorber surface.

COMSOL Simulation of temperature distribution in IT-HAG-F and IT-HAG

We have simplified the simulation by COMSOL 5.4. IT-HAG simplifies to a 30 mm ×15 mm rectangle and IT-HAG-F simplifies to a 1 mm thick film of the same size. By placing the model in water, we roughly assume that there is enough water, that the temperature does not change and the gel interface in contact with the water always maintains the initial temperature. The gel-air interface is considered to be insulated except for the upper surface. The energy given to the upper surface by solar energy is used partly for heat transfer and partly for evaporation of water. The heating of the evaporator can therefore be considered as a surface heat source. The heat flux from this source into the evaporator can be expressed as

$$Q=Q_{solar}- Q_{evap}$$

Where Q_{solar} approximate to be 950 W, and the evaporative flux can be expressed as

$$Q_{evap} = H_v k(C_{sat,G}(T) - C_e) \qquad 3$$

Where H_v, k are the heat of evaporation, and the mass transfer coefficient, respectively. $C_{sat,G}(T)$ are Vapor concentration on the surface of the gel and vapor concentration of the environment. The saturation concentration relates to the saturation pressure $p_{sat,G}$ as

$$C_{sat,G}(T) = p_{sat,G}(T)/RT$$

p_e can be calculated from

$$p_e = p_{sat.\,e} \times RH$$

where $p_{sat.\,e}$ is the saturated vapor pressure of the environment and RH is the relative humidity. Based on the conservation of energy and by applying mixing rules, the following equation is obtained for the heat transport equation

$$Q = \rho C_p \frac{\partial T}{\partial t} + \rho C_p u \cdot \nabla T + \nabla(-k \nabla T)$$

where ρ, C_p, and k are the density, heat capacity, and thermal conductivity of the medium, respectively; T represents the local temperature. In the steady state analysis of the results, all the energy not used for evaporation is lost by transferring heat to the bulk water, hence the heat loss

$$Q_{loss} = Q_{solar} - Q_{evap}$$

Cost analysis of materials and cost-effectiveness comparison of solar evaporators

All our IT-Gel-Fs were designed with cost reduction in mind. We used inexpensive graphite as the absorbent, unlike many other studies that use costly materials like graphene and carbon nanotubes. While this may slightly affect the performance of our evaporator, the price of graphite is only $1/kg, which significantly reduces costs (all prices are based on Alibaba.com). Moreover, the film's design allows for a reduced use of materials due to its extremely thin thickness, resulting in lower costs. Even at a low cost, our gels surpass most materials due to their excellent thermal management properties.

The cost of IT-HAG-F 0.3 mm: When preparing IT-HAG-F 0.3 mm gel and placing it in water, each side length increased by 1.5 times due to swelling. Therefore, to prepare a 100 cm × 100cm × 0.03 cm gel, only 66 cm × 66 cm × 0.02 cm = 87mL of solution was required. Since the gel needs to be inserted into the water at both ends, the actual length required would be greater than 100 cm. We calculated it as three times 300 cm for this purpose. A total of 198 cm × 66 cm × 0.02 cm = 261 mL of monomer solution was needed. For the solution, 6.96 g of LMA (6.1 $/kg), 13.92 g of LiCl (50 $/kg), 13.05g of graphite (1 $/kg), 60.9 g of AAm (2 $/kg), 6.09 g of SDS (1.7 $/kg), 0.435 g of BIS (8 $/kg), 0.261g of potassium persulfate (0.38 $/kg), and 0.435 mL of TEMED (ρ= 0.775 g/cm³, 9 $/kg) were required. The total cost was estimated to be 0.89 $/m².

The cost of IT-PAAmG-F 0.3mm:

Unlike IT-HAG-F 0.3 mm gel, IT-PAAmG-F had almost no volume change once prepared and placed in water. Since our gel must be inserted into the water at both ends, the actual required length would exceed 100 cm. We calculated it as three times 300 cm for a total of 900 mL of monomer solution. For this solution, 45 g of graphite (1 $/kg), 210 g of AAm (2 $/kg), 21g of SDS (1.7 $/kg), 21g of BIS (8 $/kg), 0.9 g of potassium persulfate (0.38 $/kg), and 0.45 mL of TEMED (ρ = 0.775 g/cm³, 9 $/kg) were required. The total cost was estimated to be 0.67 $/m².

S2. Supplementary Figures

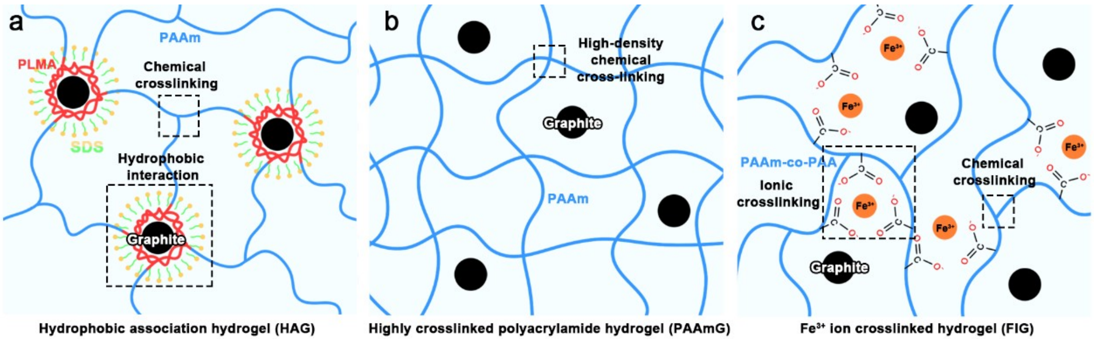

Hydrophobic association hydrogel (HAG)

Highly crosslinked polyacrylamide hydrogel (PAAmG)

Fe^{3+} ion crosslinked hydrogel (FIG)

Fig. S1 Schematic microstructure of hydrophobic association hydrogel (a), highly crosslinked polyacrylamide hydrogel (b) and Fe^{3+} ion crosslinked hydrogel (c).

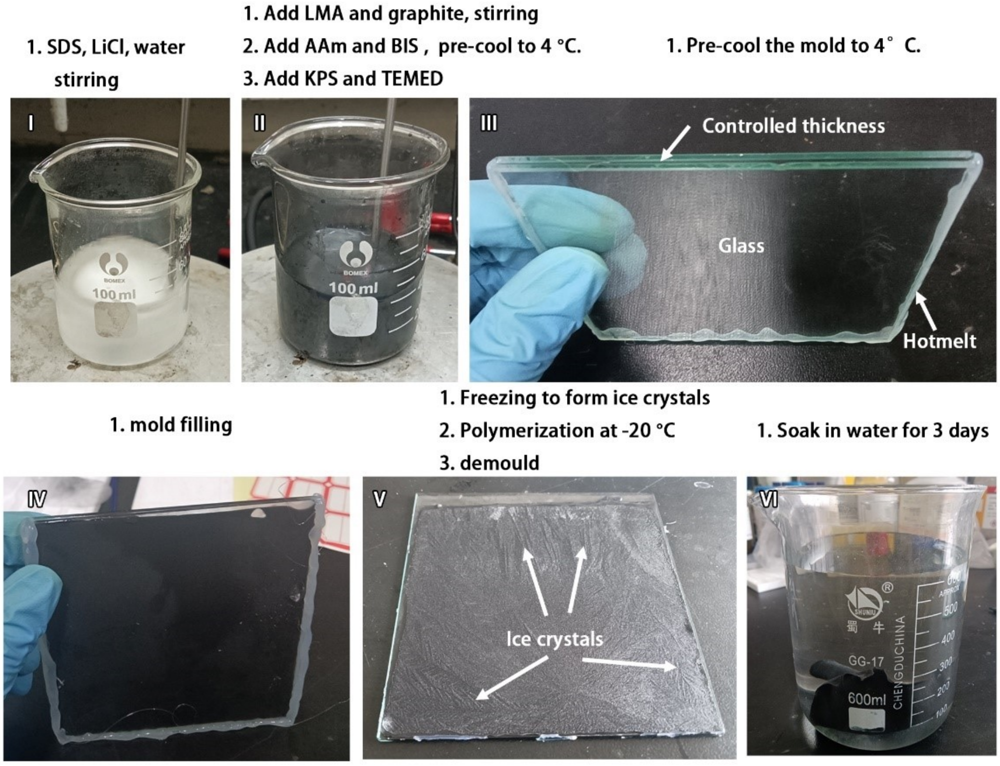
1. SDS, LiCl, water stirring

1. Add LMA and graphite, stirring
2. Add AAm and BIS , pre-cool to 4 °C.
3. Add KPS and TEMED

1. Pre-cool the mold to 4° C.

1. mold filling

1. Freezing to form ice crystals
2. Polymerization at -20 °C
3. demould

1. Soak in water for 3 days

Fig. S2 Preparation process of the IT-HAG-F.

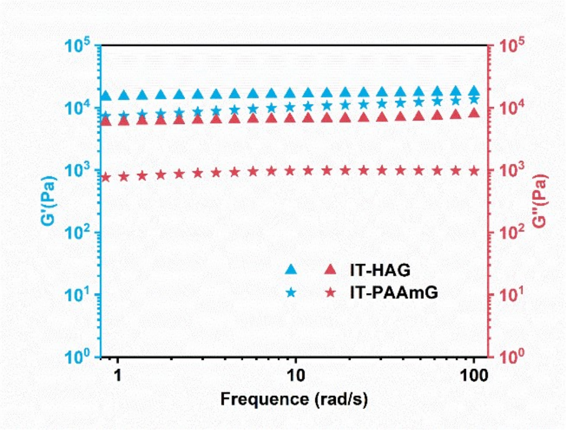

Fig. S3 Dynamic mechanical analysis of storage modulus (G′) and loss modulus (G″) of IT-HAG and IT-PAAmG.

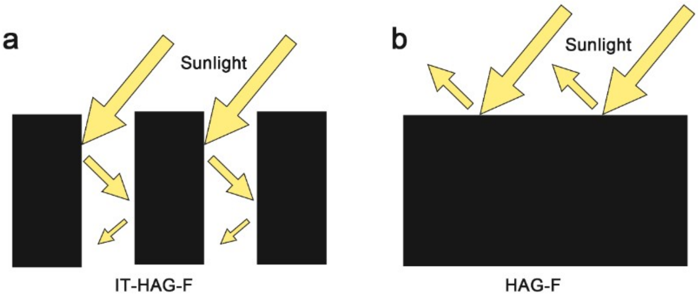

Fig. S4 Schematic diagram of the difference in light absorption properties between IT-HAG and HAG.

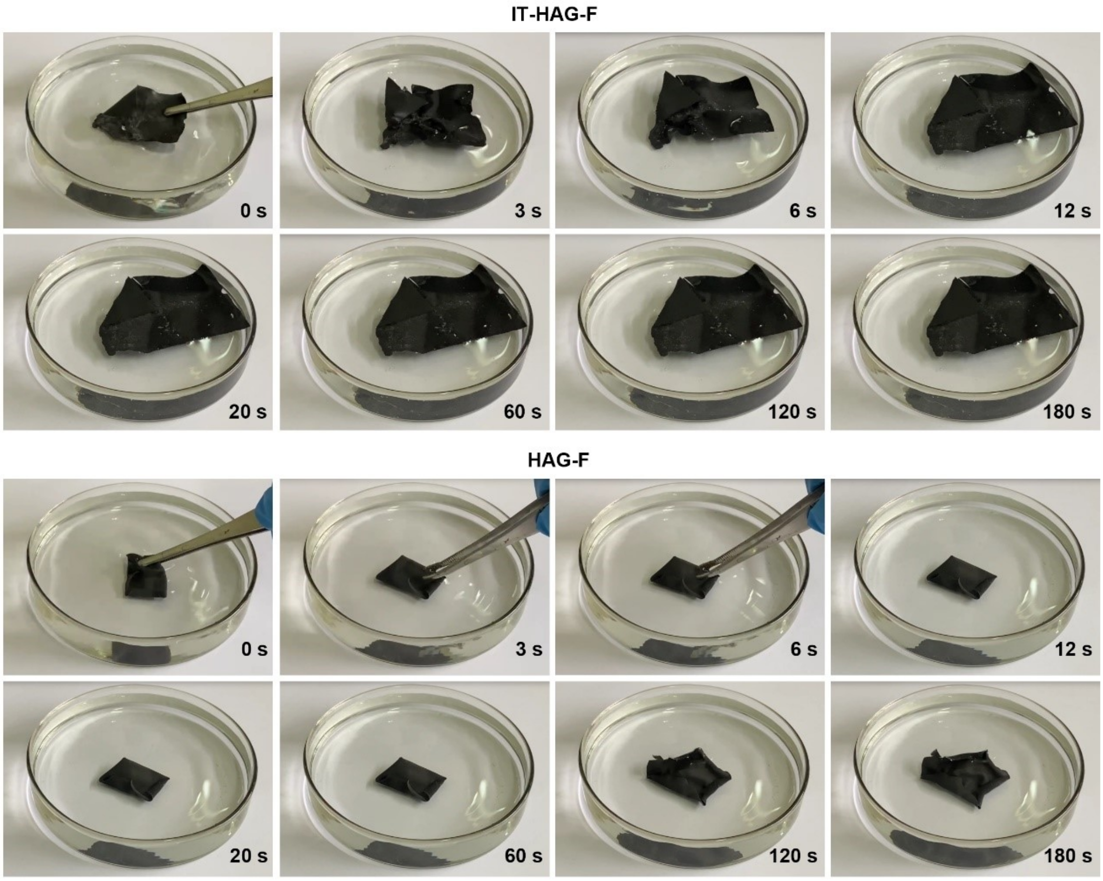

Fig. S5 Swelling process of IT-HAG-F and HAG-F in water. Images were intercepted from supplementary movie 1 and 2.

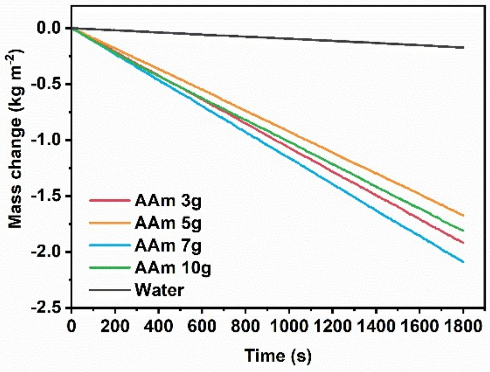

Fig. S6 Mass loss of water under 1 sun light using IT-HAG-F evaporators with different AAm contents.

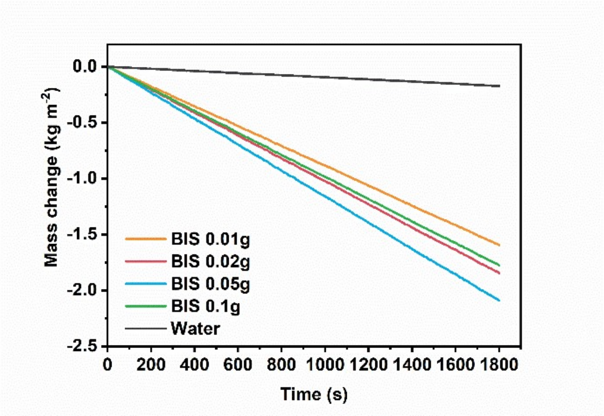

Fig. S7 Mass loss of water under 1 sun light using IT-HAG-F evaporators with different BIS contents.

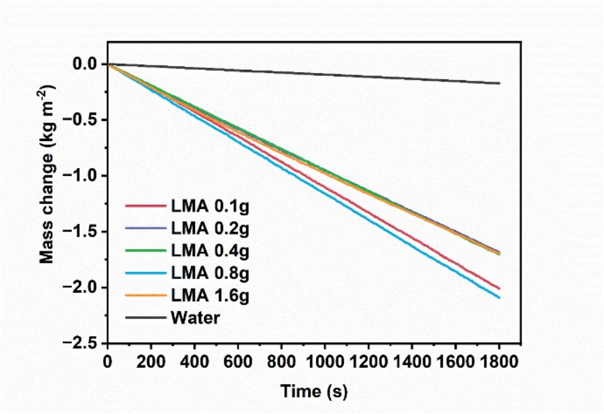

Fig. S8 Mass loss of water under 1 sun light using IT-HAG-F evaporators with different LMA contents.

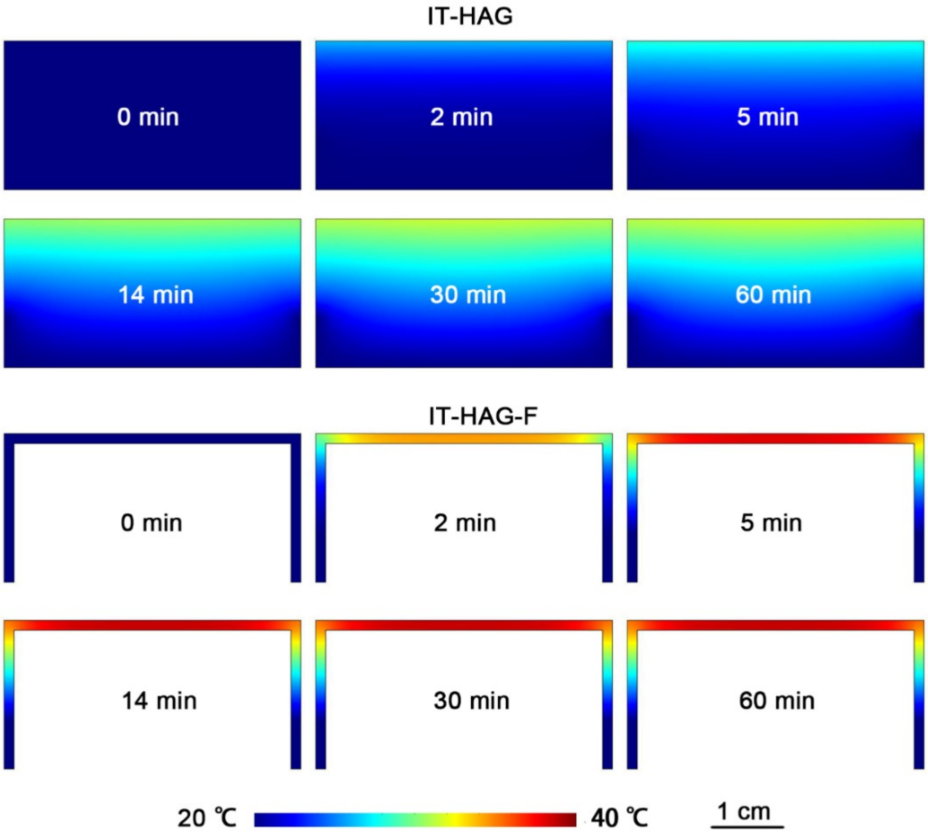

Fig. S9 Temperature distribution at different time under 1sun irradiation simulated by COMSOL.

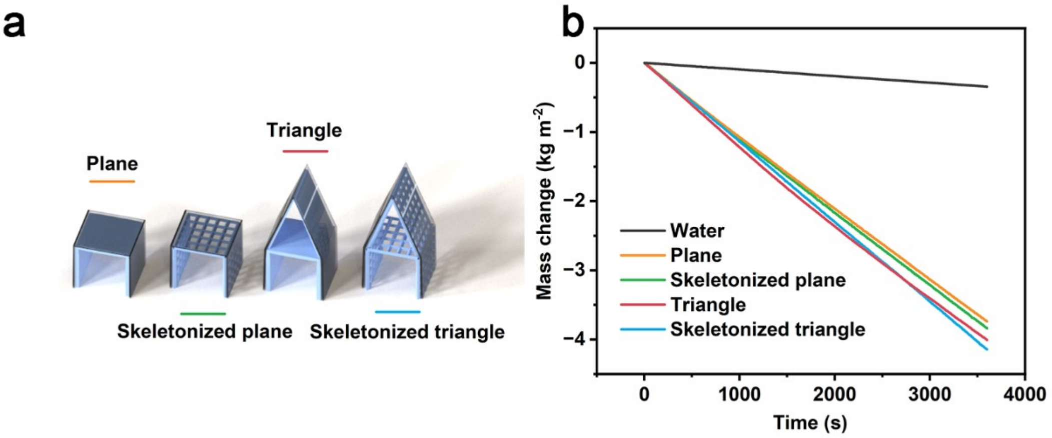

Fig. S10 Effect of evaporator morphology on evaporative performance. (a) Schematic structure of different holders used for evaporation. (b) Mass loss of water using different holders.

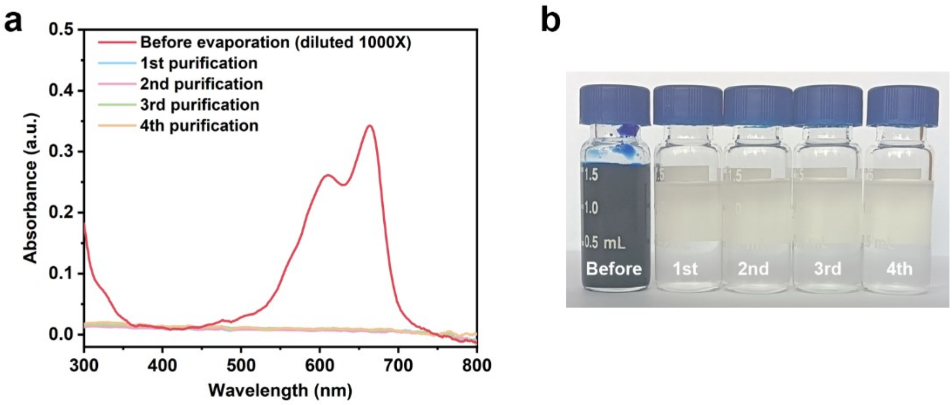

Fig. S11 Purification performance of IT-HAG-F after multiple cycles. (a) UV-VIS spectra of methylene blue solution after multiple cycles. (b) Macroscopic images of methylene blue solution after multiple cycles.

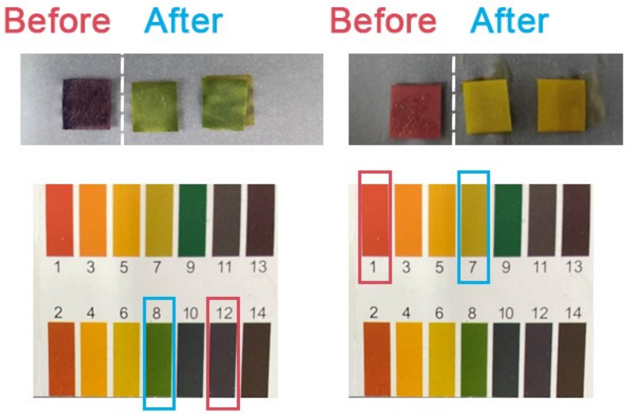

Fig. S12 Changes in pH of water before and after purification by IT-HAG-F evaporator.

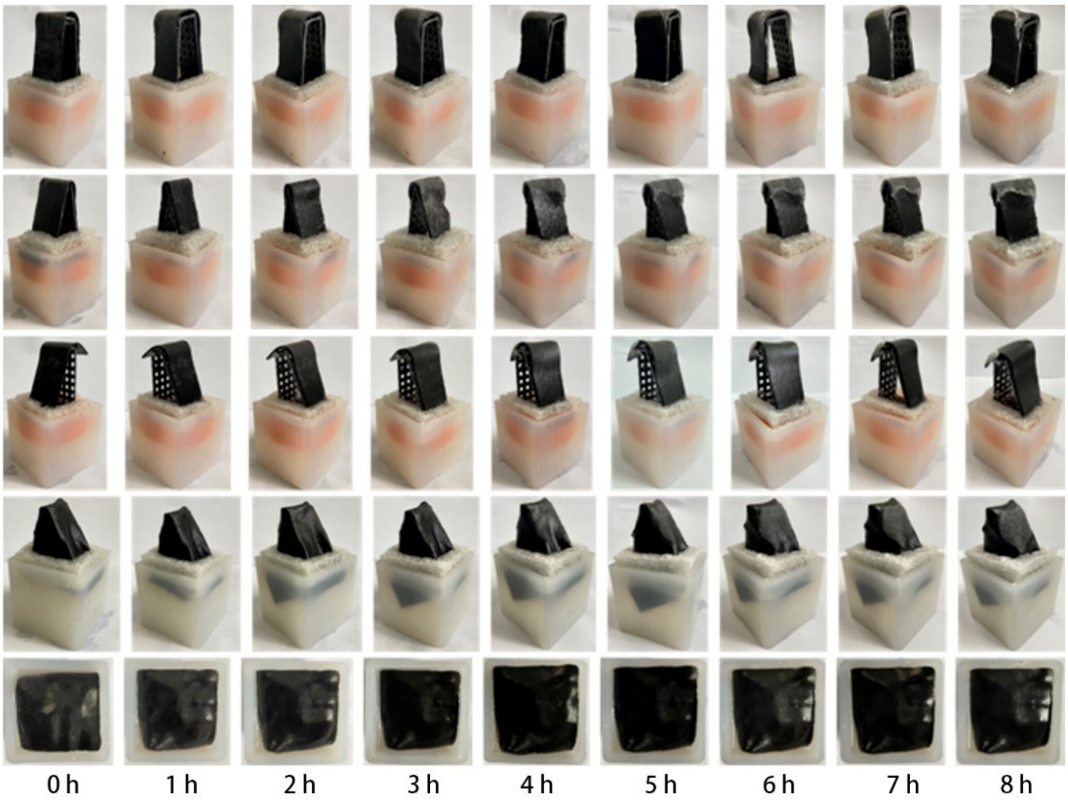

Fig. S13 Salt precipitation of different shaped IT-HAG-F when used for evaporation of 3.5 % concentration brine.

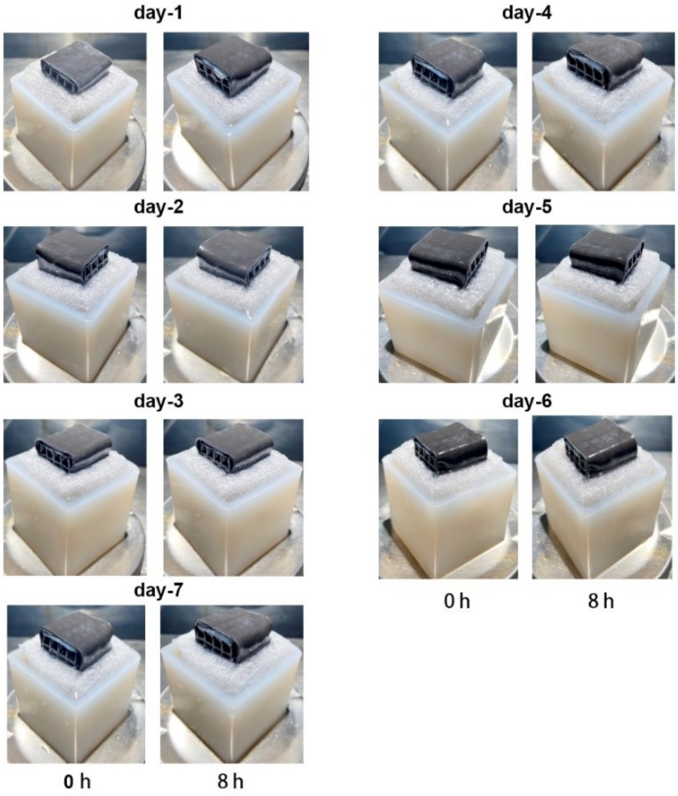

Fig. S14 Salt-resistant performance of IT-HAG-F during continuous evaporation of real seawater.

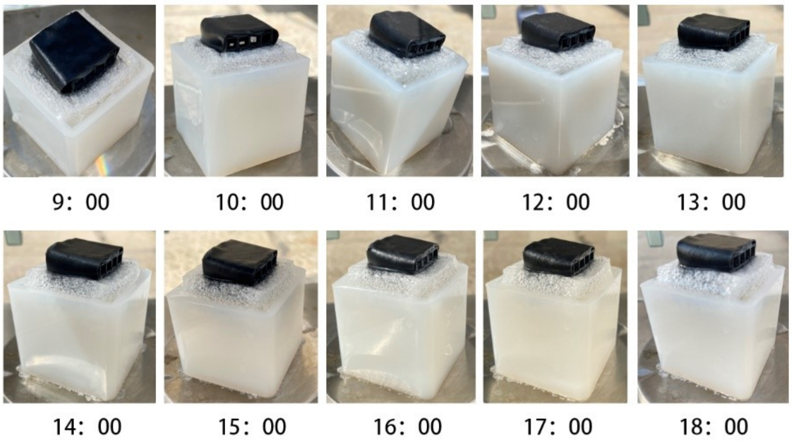

Fig. S15 Salt-resistant performance of IT-HAG-F during continuous evaporation of real seawater under natural sun irradiation.

S3. Supplementary Tables

Table S1 Comparison of cost-effectiveness over previous reported solar evaporators.

Ref	Raw Materials	Estimated single item cost ($\$/m^2$)	Total cost ($\$/m^2$)	Evaporation rate (kg m^{-2} h^{-1})	Cost effectiveness (Rate/Price, g h^{-1}/\$)
[1]	PVA Pyrrole APS	-\$13 -\$0.42 -\$0.4	13.8	3.2	231
[4]	-Polypyrene -Air-laid paper	-\$10 -\$10	20	1.35	67.5
[5]	-Ammonium persulfate (($(NH_4)_2S_2O_8$, 98%) -Hexahydroxytriphenylene (HHTP, 95%) -Copper mesh	-\$5 -\$175 -\$10	190	1.5	5
[6]	-polyvinyl alcohol (PVA) -Ti_2O_3	-\$11.60 -\$281.61	293.21	3.6	12.3
[7]	-Copper Mesh -$K_2S_2O_8$ -Fluorinated silane -Copper tube -Double-walled solar	-\$35.8 -\$0.77 -\$19.80 -\$4.34 -\$0.35	110.34	0.7	6

	vacuum tube -Polyurethane rod -Air laid paper	 -$47.26 -$2.02			
8	PVA Carbon nanofibers DMSO	-$7.7 -$8.3 -$128	144	2.53	17.5
9	Alkali lignin Hydroxyethyl cellulose Epichlorohydrin NaOH LiBr HBr	-$0.24 -$0.175 -$0.22 -$ 0.6 -$ 9.15 -$ 0.3	10.7	1.84	172
10	DMAPS NIPAM PEGDA APS TEMED Pyrrole	-$500 -$7.14 -$1.14 -$26 -$0.073 -$114	648	3.45	5.32
11	Graphene oxide L (+)-ascorbic acid Sodium alginate Acetic acid KH-560	-$550 -$24 -$30 -$19.3 -$5	628	1.85	2.95
12	2-Methylimidazole $Co(NO_3)_2 \cdot 6H_2O$ DMF PAN Sulfuric acid Nitric acid	-$0.54 -$1.8 -$27 -$7.2 -$10 -$28	74.5	3.23	43.4
13	CNTs Glutaraldehyde Hydroxypropyl cellulose	-$4 -$0.015 -$1.39	5.2	3.06	588
14	PVA sponge Ti_3AlC_2 LiF Pyrrole HCl APS	-$2 -$2.4 -$0.24 -$0.32 -$0.007 -$0.15	5.2	2.45	471
15	Activated carbon Cotton fabric Polyester pillar Expandable polyethylene	-$0.08 -$0.69 -$2 -$0.69	3.46	1.95	563

[16]	-PVA -Konjac glucomannan -MOF derived absorber	-\$7.71 -\$0.08 -\$7.15	14.9	3.2	215
Our work	LiCl AAm LMA Graphite SDS	-\$0.042 -\$0.696 -\$0.0013 -\$0.122 -\$0.010	0.87	3.84	4414
Our work	AAm Graphite BIS SDS	-\$0.42 -\$0.045 -\$0.168 -\$0.036	0.67	3.14	4687

S4. Supplementary References

1 F. Zhao, X. Zhou, Y. Shi, X. Qian, M. Alexander, X. Zhao, S. Mendez, R. Yang, L. Qu and G. Yu, *Nat. Nanotechnol.*, 2018, **13**, 489-495.

2 X. Zhou, F. Zhao, Y. Guo, Y. Zhang and G. Yu, *Energy Environ. Sci.*, 2018, **11**, 1985-1992.

3 T. Poós and E. Varju, *Int. J. Heat Mass Tran.*, 2020, **153**, 119500.

4 X. Wang, Q. C. Liu, S. Y. Wu, B. X. Xu and H. X. Xu, *Adv. Mater.*, 2019, **31**, 1807716.

5 Q. Ma, P. Yin, M. Zhao, Z. Luo, Y. Huang, Q. He, Y. Yu, Z. Liu, Z. Hu, B. Chen and H. Zhang, *Adv. Mater.*, 2019, **31**, 1808249.

6 Y. Guo, X. Zhou, F. Zhao, J. Bae, B. Rosenberger and G. Yu, *ACS Nano*, 2019, **13**, 7913-7919.

7 C. Chang, P. Tao, J. Xu, B. Fu, C. Song, J. Wu, W. Shang and T. Deng, *ACS Appl. Mater. Interfaces*, 2019, **11**, 18466-18474.

8 L. Zhang, Y. Zhang, M. Zou, C. Yu, C. Li, C. Gao, Z. Dong, L. Wu and Y. Song, *Adv. Funct. Mater.*, 2023, **33**, 2300318.

9 X. Lin, P. Wang, R. Hong, X. Zhu, Y. Liu, X. Pan, X. Qiu and Y. Qin, *Adv. Funct. Mater.*, 2022, **32**, 2209262.

10 C. Lei, J. Park, W. Guan, Y. Zhao, K. P. Johnston and G. Yu, *Adv. Funct. Mater.*, 2023, **33**, 2303883.

11 H. Ma, L. Yu, Z. Li, J. Chen, J. Meng, Q. Song, Y. Liu, Y. Wang, Q. Wu, M. Miao and C. Zhi, *Small*, 2023, **19**, 2304877.

12 R. Zhang, B. Xiang, Y. Wang, S. Tang and X. Meng, *Mater. Horiz.*, 2022, **9**, 1232-1242.

13 Z. Wang, R. Jin, S. Zhang, X. Han, P. Guo, L. Jiang and L. Heng, *Adv. Funct. Mater.*, 2023, **33**, 2306806.

14 Y. Pan, E. Li, Y. Wang, C. Liu, C. Shen and X. Liu, *Environ. Sci. Technol.*, 2022, **56**, 11818-11826.

15 Q. Zhang, R. Hu, Y. Chen, X. Xiao, G. Zhao, H. Yang, J. Li, W. Xu and X. Wang, *Appl. Energy*, 2020, **276**, 115545.

16 Y. Guo, H. Lu, F. Zhao, X. Zhou, W. Shi and G. Yu, *Adv. Mater.*, 2020, **32**, 1907061.